were significantly higher in MGT-treated mice than those of the vehicle control. Taken together with our previous data, it is suggested that inflammatory responses might be involved in the genotoxicity induced by MGT in the lungs of mice.

**Keywords:** magnetite nanoparticle; pulmonary inflammation; intratracheal instillation; DNA adductome

## 1. Introduction

Magnetite nanoparticles (MGT) have been widely utilized in medicinal and industrial fields [1]. Moreover, in medical applications, MGTs are widely used for magnetic resonance imaging as a contrast agent based on their good bio-compatibility [2,3]. With increasing utilization of MGT, it has been a concern whether MGTs are safe for humans or not. Hitherto, several reports describing MGT toxicity have been published [4–13], however, there is still controversy over reports regarding toxicity. Most investigations are focused on studying effects of MGTs on *in vitro* cellular viability, morphology and metabolism, or *in vivo* general toxicity on various organs with various administration routes of MGT (intraperitoneal, intratracheal or intravenous injection). Recently, we have reported genotoxic effects of MGTs using *in vitro* and *in vivo* assay systems, and clearly demonstrated that MGTs induce genotoxicity in both cultured mammalian cells and mice lungs instilled intratracheally [14–16]. Based on mutation spectra, histopathological evaluation, and oxidative- and lipid peroxide-related DNA adduct formations, it is suggested that inflammatory responses might contribute to the genotoxicity induced by MGT treatment [16].

It is well known that DNA adducts are considered to be triggers for induction of gene mutations [17–21]. In our previous report, MGT predominantly induced a C to T transition in mouse lungs [16]. Levels of 8-oxo-7,8-dihydro-2'-deoxyguanosine (8-oxodG) and heptano-etheno (Hε)-adducts were also elevated in lungs of mice exposed to MGT [16]. Although Hε-dC induces C to T transitions *in vitro* [22,23], the mechanisms of genotoxicity induced by MGT are not fully explained yet. Global discovery of DNA adducts in target organs would be useful information for exploring the mechanisms of genotoxicity.

Recently, Kanary *et al.* [24,25], established a method consisting of liquid chromatography followed by double tandem mass spectrometry for comprehensive analysis of DNA adducts in human and animal tissues. The basic strategy is designed to detect the neutral loss of a 2'-deoxyribose moiety [M + H; −116] from positively ionized 2'-deoxynucleoside adducts in multiple reaction ion monitoring mode (MRM) transmitting the precursor ion [M + H] ≥ daughter ion [M + H; −116] [24]. Using this method, hundreds of DNA adducts can be detected at once. Based on this strategy, we recently established comprehensive analysis of DNA adducts by using a UPLC-QTOF mass spectrometer. In this method, $MS^E$ analysis was used to detect the neutral loss of a 2'-deoxyribose moiety [M + H; −116.04736]. Using this method, accurate mass values of precursor ions can be obtained, and this is an advantage for identification of chemical structures of DNA adducts. To identify the chemical structures of DNA adducts screened by adductome analysis, we have already made a list of DNA adducts, including *m/z* [M + H] values of precursor and daughter ions corresponding to more than 250 literature-based DNA

adducts (see additional file 3). Moreover, the data obtained from *in vitro* model reactions such as oxidative stress, inflammation and alkylation are also included in this list. To clarify the mechanisms involved in genotoxicity induced by MGT, here, we examined the comprehensive DNA adduct analysis (DNA adductome analysis) of mice lungs exposed to MGT.

## 2. Results and Discussion

### *2.1. Comprehensive Analysis of DNA Adducts Induced by MGT (Nanosized-Magnetite) Treatment*

Recently, we have reported that MGT clearly demonstrated genotoxicity in the lungs of *gpt* delta transgenic mice after intratracheal instillation [16]. As a result of mutation spectra analysis, most mutations induced by MGT occurred at G:C base pairs, and the prominent mutation types were a G:C to A:T transition followed by a G:C to T:A transversion [16].

To investigate mechanisms of the induction of mutations in mouse lungs by MGT exposure, we performed comprehensive analysis of DNA adducts according to the methods described in "Experimental Section". Totally, 30 and 42 types of DNA adducts were detected in the vehicle control and MGT-treated groups, respectively (Figure 1, and Additional File 1). Among them, 27 types of adducts were specific for the MGT-treated group, whereas 15 types of adducts overlapped between the MGT-treated and control groups.

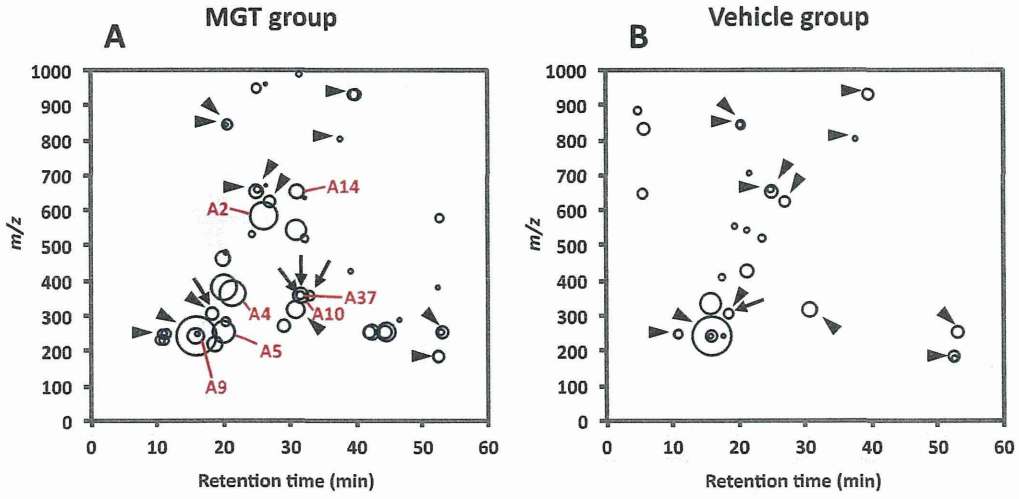


**Figure 1.** Comprehensive DNA adducts analysis. Map views of DNA adducts in lungs of mice with (**A**) or without MGT-exposure (**B**). Arrow heads indicate the DNA adducts observed in both MGT and vehicle groups, and arrows indicate the corresponding DNA adducts observed in *in vitro* model reactions, including oxidized arachidonic acid, oxidized linoleic acid or hydroxy radical with ctDNA (see additional files 1 and 3). The 7 major contributors determined by PCA and RF analyses are indicated by A2, A4, A5, A9, A10, A14 and A37, respectively.

Principal component analysis (PCA) against a subset of DNA adducts observed in these data set was further applied and is shown in the 2D PCA scores plot (Figure 2A) and associated loadings plot (Figure 2B). A clear clustering of the data could be visualized according to vehicle control and

MGT-treated mice (Figure 2A). The DNA adduct named A5 (*m/z* 252.11 [M + H] at $t_R$ 20.1 min) had the highest contribution to MGT exposure based on its PCA significance. This was followed by DNA adducts named A4 (*m/z* 363.17 [M + H] at $t_R$ 25.9 min), A10 (*m/z* 355.23 [M + H] at $t_R$ 31.0 min), A14 (*m/z* 652.37 [M + H] at $t_R$ 21.4 min) and A9 (*m/z* 243.12 [M + H] at $t_R$ 31.0 min) revealed higher contribution to MGT exposure (Figure 2B). On the other hand, the DNA adduct named A1 demonstrated the highest contribution to the vehicle control. To confirm the results from PCA analysis, a random forest (RF) analysis of the DNA adductome profile data was also performed. The DNA adducts effectively separated the groups (vehicle *vs.* MGT) and are shown in the importance plot (Additional File 1). Several DNA adducts, including A5, A10 and A14, were the most important variables causing the clustering in both mean decrease in accuracy and mean decrease in Gini index (Additional File 1). A hierarchical clustering was analyzed on the dataset consisting of the DNA adducts diagnosed as highly contributing to MGT exposure, including A5 and A10, which were selected from both PCA and RF analyses. As shown in Figure 3, the heatmap for all contributors showed a clear separation of the MGT-treated group from the vehicle control. Among these, A5 was highly correlated with MGT treatment, whereas other contributors, such as A9, A14, A10, A2 and A4 seemed to not always correlate with MGT status. On the other hand, A37 also demonstrated a clear relation with MGT status, however the abundance was lower than that of A5.

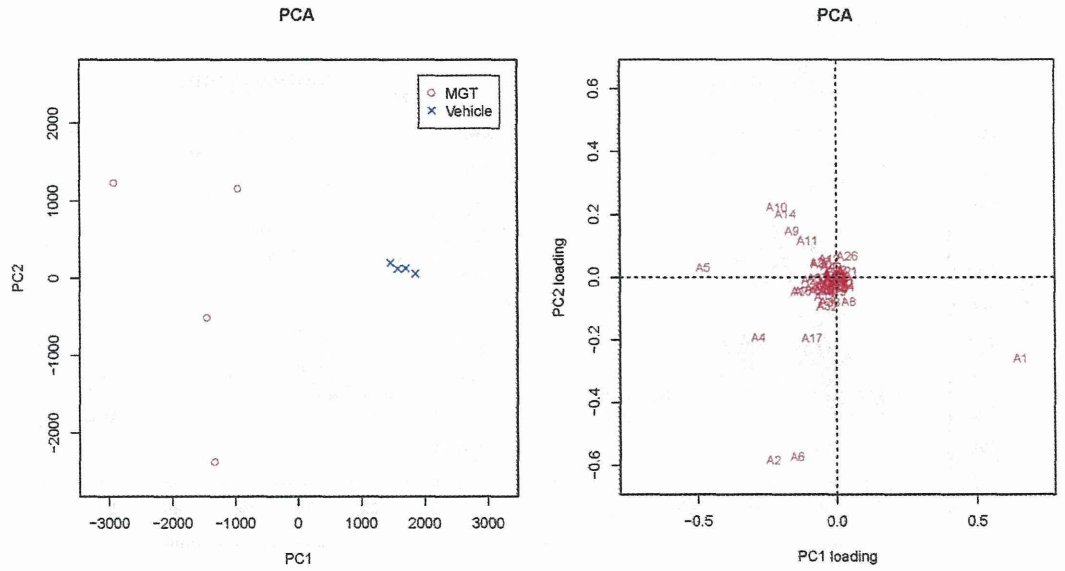


**Figure 2.** PCA scores and loading plots. (**A**) 2D PCA scores of DNA adducts obtained from adductome analysis. Principal components PC1 and PC2, which explains 74.25% of the total variance observed, discriminate the MGT-treated group from the vehicle control; (**B**) The PC1 and PC2 variable loading plots. Numbers A1–A53 represents DNA adducts observed in DNA adductome analysis.

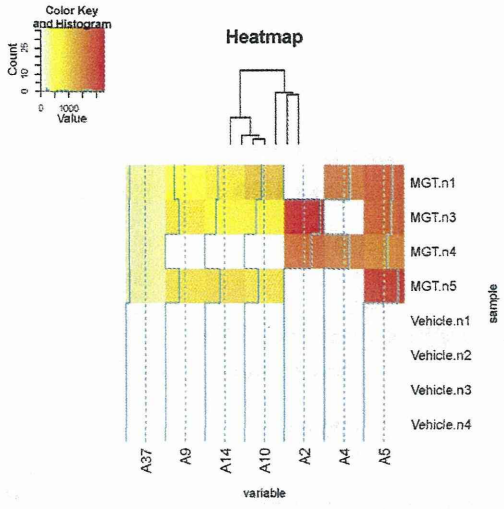


**Figure 3.** Heatmaps and clustering dendrogram. Hierarchical clustering was performed using 7 major contributors selected by PCA and RF analyses.

### *2.2. Identification of DNA Adducts Correlated with MGT Treatment*

To identify the chemical structure of DNA adducts detected as the "major contributors" to MGT status, we used the list of DNA adducts constructed by ourselves (Additional File 3). Firstly their values of *m/z* [M + H] were compared with known DNA adducts listed in Additional File 3. Among seven major contributors, A4, A5 and A9 indicated identical *m/z* values [M + H] for inflammation-related adducts, ammonium added butano-etheno-deoxyadenosine (BεdA-$NH_3$, *m/z* 363.1816 [M + H]), etheno-deoxycytidine (εdC, *m/z* 252.0984 [M + H]) and 3-methyldeoxycytidine (3-medC, *m/z* 243.1213 [M + H]), respectively. In contrast to this, we could not find identical *m/z* values [M + H] for the remaining 4 contributors in the DNA adduct list. In order to clarify the formation mechanism of the remaining 4 contributors, A2, A10, A14 and A37, we prepared various *in vitro* model reactions, including oxidative stress and inflammation, and compared their *m/z* values [M + H] and $t_R$ with each other. As a result, A10 (*m/z* 355.23 [M + H] at $t_R$ 31.5 min) and A37 (*m/z* 356.24 [M + H] at $t_R$ 31.4 min) were seen to correspond to one of the DNA adducts observed in the reaction mixture with oxidized-arachidonic acid (Additional Files 1 and 2). No adducts having *m/z* 580.79 [M + H] at $t_R$ 25.9 min (A2) and *m/z* 652.37 [M + H] at $t_R$ 31.0 min (A14) could be seen in any of the *in vitro* model reactions. From these observations, it is suggested that inflammatory responses might exist in the mechanisms behind the increase in mutations by MGT treatment.

### *2.3. Confirmation of DNA Adducts Correlated with MGT Treatment*

In order to confirm the chemical structure of DNA adducts diagnosed as highly contributing to MGT status, we synthesized authentic 15N-εdC and analyzed it by quantitative LC-MS/MS apparatus (Waters 2795 LC system interfaced with a Quattro Ultima triple stage quadrupole MS, (Waters, Manchester, UK)). A peak with a 252.1 $\geq$ 136.1 transition corresponding to εdC, eluted at the same position as authentic 15N-εdC (255.1 $\geq$ 139.1), was observed in the lungs of both vehicle and MGT-treated mice (Figure 4). Levels of εdC were significantly higher in the MGT-treated group than those of the vehicle control (Figure 4).

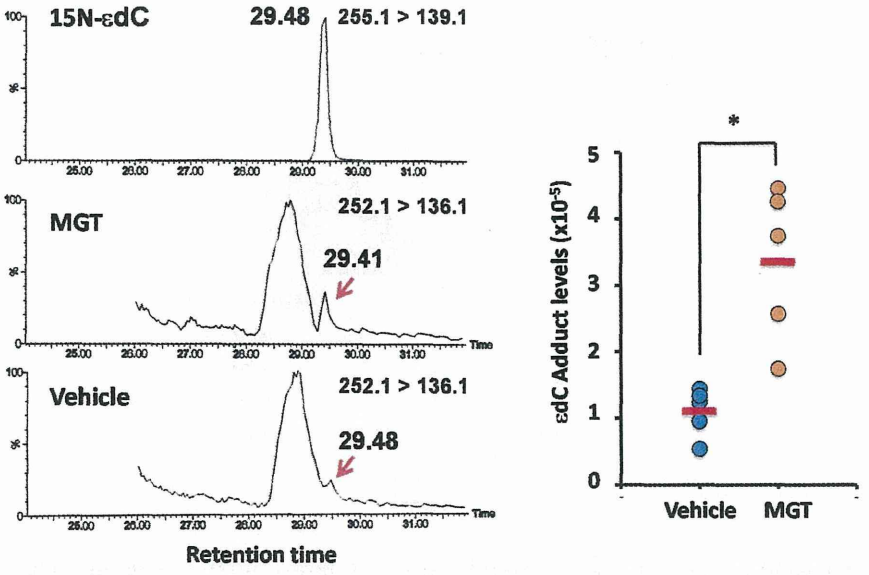


**Figure 4.** Quantitative Analysis of εdC by LC-MS/MS. εdC formation was induced by MGT exposure in the lungs of ICR mice. DNA was extracted from the lungs 24 h after intratracheal instillation of 0.2 mg per animal of MGT, and was digested enzymatically. Control samples were obtained from the lungs of mice given the vehicle for the same durations of MGT exposure. εdC were quantified by stable isotope dilution liquid chromatography-mass spectrometry (LC-MS/MS). Asterisk (*) indicates a significant difference ($p < 0.05$) from vehicle control (treatment with 0.05% (*v*/*v*) Tween-80) in the Student's *t*-test.

εdC is produced from 4-hydroperoxy-2-nonenal via lipid peroxidation, and is known to be an inflammation-related adduct [22]. Since it has been reported that εdC is involved in C to T transitions using *in vitro* assay [23], it is likely that inflammatory responses might exist in the mechanisms behind the increase in mutations by MGT treatment. Although no data are available regarding the pulmonary inflammation generated by MGT single dose exposure in the present study, we have previously demonstrated that increasing oxidative stress and inflammation-related DNA adducts, including 8-oxodG and HεdC in the lungs of MGT-treated mice [16]. In addition, ROS production and overexpression of heme oxygenase-1, which mediates an anti-inflammatory effect, were clearly observed in MGT-exposed human lung epithelial cells, A549 [14]. Supporting our hypothesis, Park *et al.* [26], have been reported that single intratracheal instillation of magnetite increased the concentration of pro-inflammatory cytokines, such as TNF-α and IL-6, in the cells of bronchoalveolar lavage (BAL) fluid after 24 h exposure. Therefore, in the present study, it is reasonable to consider that inflammatory response evoked from the host reaction against foreign bodies, MGT, induce formation of inflammation-related DNA adducts, such as εdC and HεdC, which, being involved in C to T transitions, are more likely to contribute to genotoxicity observed in the lungs of MGT-exposed mice. Recently, several reports show that the mechanisms of (geno)toxicity induced by nanoparticles are suggested to be involved in macrophage stimulation [26–33]. Innate immune activation through Nalp3 inflammasomes has been suggested to play an important role in the pulmonary inflammation and fibrotic disorders of silicosis and asbestosis [31,32]. He *et al.* [29], demonstrated that multi walled

carbon nanotubes (MWCNTs) directly induce inflammatory cytokines and chemokines, including TNF-α, IL-1β, IL-6, and MCP1 in murine macrophage cell line RAW264.7. Therefore, it is suggested that MGT can activate alveolar macrophage in the same way, then damage adjacent alveolar epithelial cells via cytokine and chemokine activation. In contrast, it has not been ruled out that direct toxicity against alveolar cells might be partly involved in induction of *in vivo* genotoxicity. It has been reported that MWCNTs damaged mitochondria to increase ROS production and cause toxicity against lung alveolar epithelial cells, A549 [29]. Similarly, we also have recently reported that MGT actually manifests cytotoxicity and clastogenicity in cultured mammalian cells [14,15]. Taken together, MGT elicits multiple events such as oxidative stress and inflammatory cytokine production, then leads to genotoxicity in mice lungs.

## 3. Experimental Section

### *3.1. Materials*

MGT was purchased from Toda Industrial Co., Ltd. (Hiroshima, Japan), and this material was identical to those used in the *gpt* delta mouse study of Totsuka *et al.*, 2014 [16]. The declared primary particle size of MGT was 10.0 nm diameter around. The surface area was 125 $m^2/g$ (disclosed by Toda Industrial Co., Ltd.). Detailed information, such as particle appearance, dispersed diameter and zeta potential of MGT can be found in the previous report [16].

### *3.2. Chemicals*

NucleaseP1 and HPLC grade methanol were purchased from Wako (Tokyo, Japan). Phosphodiesterase I was purchased from Worthington. Bovine spleen phosphodiesterase II, DNase I, Type I agarose, low melting point agarose, and Triton X-100 and bacterial alkaline phosphatase Type III (*E. coli*) were purchased from Sigma Co. (St. Louis, MO, USA). All other chemicals used were of analytical grade and purchased from Wako.

### *3.3. Animals*

Male ICR mice (6 weeks old) were obtained from Japan SLC (Shizuoka, Japan). Animals were provided with food (CE-2 pellet diet, CLEA Japan, Inc., Tokyo, Japan) and tap water *ad libitum* and quarantined for one week. Mice were maintained under controlled conditions: 12 h light/dark cycle, 22 ± 2 °C room temperature, and 55% ± 10% relative humidity. The experiments were conducted according to the "Guidelines for Animal Experiments in the National Cancer Center" of the Committee for Ethics of Animal Experimentation of the National Cancer Center.

### *3.4. Analysis of DNA Adducts*

For DNA adduct analyses, each group of 4 to 5 male ICR mice was intratracheally instilled with MGT at a single dose of 0.2 mg per animal, and sacrificed 24 h after MGT administration. Our previous study [16] demonstrated that *gpt* mutation frequency was significantly increased in mice lungs treated with multiple doses of 0.2 mg, but not in the 0.05 mg treatment group. In the DNA

adduct formation analysis, even though singly treated with 0.2 mg of MGT, the levels of oxidative stress related DNA adducts were significantly increased. Therefore, we thought that a single dose of 0.2 mg MGT/animal was sufficient to analyze comprehensive DNA adduct analysis. Control samples were obtained from the lungs of mice given the vehicle. Mouse lung DNA was extracted and purified using a Gentra® Puregene™ tissue kit (QIAGEN, Valencia, CA, USA). The protocol was performed according to the manufacturer's instructions except that desferroxamine (final concentration: 0.1 mM) was added to all solutions to avoid the formation of oxidative adducts during the purification step. The extracted DNA was stored at −80 °C until analysis for DNA adductome analysis.

#### 3.4.1. Comprehensive Analysis of DNA Adducts (DNA Adductome Analysis)

Mouse lung DNA extracted from vehicle ($n$ = 4) and MGT treated ($n$ = 4) mice were enzymatically digested according to the method of Goodenough *et al.* [24], with some modifications. Briefly, internal standards (2',3'-dideoxyinosine and 2',3'-dideoxyguanosine) were added to the DNA solution prior to enzyme digestion, at 12.7 nM. The enzymatic digestion conditions are as follows; DNA (67 μg) in 5 mM Tris-HCl buffer (pH 7.4) employed DNase I (Type IV from bovine pancreas) for 3 h. Next, nuclease P1 (from *Penicillium citrinum*), 10 mM sodium acetate (pH 5.3, final 10 mM), and $ZnCl_2$ (final 34 mM) were added, and incubated for a further 3 h at 37 °C. Alkaline phosphatase (from *E. coli*), phosphodiesterase I (20 U/mL in water) and Tris base (final 15.4 mM) were added last, for an additional 16–18 h at 37 °C. The sample was purified using Vivacon500® (10 kDa molecular weight cut-off filters, Sartorius AG, Goettingen, Germany), then, the reaction mixture was centrifuged (4 °C, 10,000× $g$, 15 min) using Ultrafree® (0.2 μm pore; Millipore Co., Billerica, MA, USA) and the filtrate was used for DNA adductome analysis.

LC-MS analyses were performed using a nanoACQUITY UPLC system (Waters, Milford, MA, USA) equipped with a Xevo QTOF mass spectrometer (Waters, Manchester, UK), instrumented with an electrospray ionization source (ESI) and controlled by MassLynx 4.1 software. Sample injection volumes of 4 μL each were separated on a ACQUITY UPLC BEH130 C18 column (1.7 μm, 1.0 mm i.d. × 150 mm) at a flow rate of 25 μL/min. The column temperature was set to 40 °C. Mobile phase A and B were water and methanol, respectively. Chromatographic separation was performed by a gradient elution as follows: 0–5 min, 1% B; 5–10 min, linear gradient to 10% B; 10–35 min, linear gradient to 80% B; 35–45 min, 80% B. MS parameters were set as follows: mass range scanned from 50 to 1000 with a scan duration of 0.5 s (1.0 s total duty cycle), capillary 3.7 kV, sampling cone 40 V, extraction cone 4 V, source temperature 125 °C, desolvation temperature 250 °C. Nitrogen gas was also used as the desolvation gas (flow 800 L/h) and cone gas (30 L/h). All data were collected in positive ion mode. $MS^E$ analysis was performed on the mass spectrometer set at 3 V for low collision energy and ramp of 10–25 V for high collision energy during the acquisition cycle. A cone voltage of 20 V was used. LockMass parameters were set as following: capillary 3.0 kV, sample cone 40 V, collision energy 21 V.

Relative peak intensity of each potential DNA adduct was calculated as previously described [33]. The relative peak intensity was plotted as a bubble chart in which the horizontal axis was retention time and the vertical axis was $m/z$. DNA obtained from normal human fetal fibroblast cell line, TIG-3, with internal standard was used as a reference [33].

3.4.2. Data Processing

The raw data files obtained from LC/MS runs were analyzed using MassLynx v4.1 and MarkerLynx 4.1 software (Waters). The application detects, integrates, and normalizes the intensities of the peaks to the sum of peaks within the sample. The resulting multivariate dataset consisting of the peak number (based on the retention time and *m/z*), sample name, and the normalized peak intensity was analyzed by S-plot analysis using SIMCA-P+ 11.5 (Umetrics AB, Umea, Sweden). The method parameters were as follows: Mass tolerance = 0.05 Da, Apex Track Parameters: Peak width at 5% height (seconds) = 15/Peak-to-peak baseline noise = 50, Apply smoothing = Yes, Collection Parameters: Intensity threshold (counts) = 100/Mass window = 0.05/Retention time window = 0.10, Noise elimination level = 6, Deisotope data = Yes.

3.4.3. *In Vitro* Modification of DNA

The DNA modification derived from oxidation of unsaturated fatty acids was performed by incubating calf thymus DNA (ctDNA, 1 mg/mL, Sigma, Steinheim, Germany) with 20 mM unsaturated fatty acids including arachidonic acid (Sigma) and linoleic acid (Sigma) in the presence of 75 μM $CuSO_4$ (Wako) and 1.5 mM ascorbic acid (Wako). The DNA modification related to oxidative stress was formed from ctDNA and 10 mM hydrogen peroxide (Wako) in the presence of 1 mM $CuSO_4$ and 1 mM ascorbic acid in 1 mL of 500 mM sodium phosphate buffer, pH 7.4 for 24 h, in atmospheric oxygen at 37 °C. The reaction was terminated by the addition of 1 mM butylated hydroxytoluene (Wako) and 100 μM diethylenetriaminepentaacetic acid (Wako).

3.4.4. Confirmation of εdC

Mouse lung DNA (40 μg) extracted from vehicle ($n$ = 5) and MGT treated ($n$ = 5) mice was enzymatically digested, and εdC was analyzed and quantified by the Waters 2795 LC system (Waters, Manchester, UK) interfaced with a Quattro Ultima triple stage quadrupole MS (Waters) using the same procedure previously described [34]. Authentic 15N-εdC was kindly provided by Dr. Yoshitaka Matsushima (Tokyo University of Agriculture) synthesized according to previously published methods [35]. The multiple reaction monitoring transitions were monitored; each cone voltage and collision energy used were εdC [252.1 ≥ 136.1, 35 V, 10 eV].

*3.5. Statistical Analysis*

PCA and RF analyses were used for modeling comprehensive analysis of DNA adducts (DNA adductome analysis). All the calculations were performed using statistical package R. In RF, we confirmed that the out-of-bag misclassification rate was saturated at 0% with 100,000 generated trees with two variables. The data were statistically compared with the corresponding solvent control using the Student's $t$ test for DNA adduct formation. The data were compared with the corresponding solvent control using the F test before application of the Student's $t$ test. If the F test evaluation showed an unequal variance, the $p$ value was determined using the Welch's $t$ test.

## 4. Conclusions

We have demonstrated that MGTs induce inflammation-related DNA adduct formation in mouse lungs by using comprehensive analysis of DNA adducts, DNA adductome analysis. In PCA analysis, εdC was detected as the "major contributor" to MGT status. Due to the inducible base, the exchange pattern of εdC has been reported to be a C to T transition [22.23], being the predominant mutational pattern detected in mouse lungs exposed to MGT [16]. Therefore, it is suggested that inflammatory responses lead to inflammation-related DNA adduct formations, such as εdC, and this might contribute to the genotoxicity in mouse lungs induced by MGT treatment.

## Acknowledgments

We thank Naoaki Uchiya, Yoko Matsumoto and Akihiro Sekine for their excellent technical assistance. This study was supported by Grants-in-Aid for Cancer Research, for the U.S.-Japan Cooperative Medical Science Program, for Research on Risk of Chemical Substances from the Ministry of Health, Labor, and Welfare of Japan, for Young Scientists (B) 23710084 from the Ministry of Education, Culture, Sports, Science and Technology of Japan. The study was also supported by a grant from the Japan Chemical Industry Association (JCIA) Long-range Research Initiative (LRI). Kousuke Ishino was the recipient of a Research Resident Fellowship from the Foundation for Promotion of Cancer Research.

## Author Contributions

Kousuke Ishino, Yukari Totsuka and Tatsuya Kato performed DNA adducts analysis and drafted the manuscript. Mamoru Kato carried out statistical analysis. Analysis of size distribution and agglomeration state of particles were done by Masatoshi Watanabe. Tatsuhiro Shibata, Keiji Wakabayashi and Hitoshi Nakagama conceived and supervised the study. All authors read and approved the final manuscript.

## Appendix

**Additional File 1.** List of the data set obtained from DNA adductome analysis.

| Peak No. | RT (min) | *m/z* | Area Mean ± SD | | *p*-Value (*t* Test) | Fold Change |
|---|---|---|---|---|---|---|
| | | | MGT | Vehicle | | |
| 1 | 16.0 | 242.11 | 4867 ± 722 | 4938 ± 2414 | 0.485 | 0.99 |
| 2 | 25.9 | 580.79 | 2389 ± 837 | - | - | - |
| 3 | 21.4 | 363.17 | 2016 ± 850 | - | - | - |
| 4 | 20.1 | 252.11 | 1543 ± 375 | - | - | - |
| 5 | 31.0 | 543.33 | 1273 ± 732 | - | - | - |
| 6 | 44.4 | 252.11 | 1099 ± 669 | - | - | - |
| 7 | 30.9 | 317.17 | 957 ± 125 | 676 ± 363 | 0.294 | 1.41 |
| 8 | 16.0 | 243.12 | 775 ± 112 | - | - | - |
| 9 [a] | 31.5 | 355.23 | 758 ± 221 | - | - | - |

**Additional File 1.** *Cont.*

| Peak No. | RT (min) | *m/z* | Area Mean ± SD | | *p*-Value (*t* Test) | Fold Change |
|---|---|---|---|---|---|---|
| | | | MGT | Vehicle | | |
| 10 | 18.8 | 219.11 | 703 ± 819 | - | - | - |
| 11 | 20.0 | 463.73 | 677 ± 504 | - | - | - |
| 12 | 31.0 | 652.37 | 632 ± 249 | - | - | - |
| 13 | 25.0 | 655.40 | 591 ± 188 | 493 ± 39 | 0.106 | 1.20 |
| 14 | 28.9 | 273.18 | 491 ± 205 | - | - | - |
| 15 | 41.8 | 252.11 | 471 ± 111 | - | - | - |
| 16 [c] | 18.4 | 308.13 | 468 ± 129 | 293 ± 27 | 0.010 | 1.59 |
| 17 | 53.0 | 252.11 | 458 ± 182 | 455 ± 162 | 0.447 | 1.03 |
| 18 | 52.5 | 181.98 | 415 ± 167 | 387 ± 156 | 0.425 | 1.07 |
| 19 | 26.9 | 622.79 | 411 ± 132 | 349 ± 110 | 0.287 | 1.18 |
| 20 | 39.7 | 928.61 | 379 ± 137 | 384 ± 83 | 0.490 | 0.99 |
| 21 | 20.2 | 841.27 | 317 ± 310 | 259 ± 179 | 0.452 | 1.23 |
| 22 | 11.0 | 230.11 | 295 ± 82 | - | - | - |
| 23 [b] | 32.9 | 360.21 | 269 ± 98 | - | - | - |
| 24 | 25.0 | 946.44 | 265 ± 154 | - | - | - |
| 25 | 20.2 | 284.13 | 252 ± 34 | - | - | - |
| 26 | 10.9 | 250.08 | 252 ± 70 | 264 ± 135 | 0.176 | 0.95 |
| 27 | 52.5 | 575.30 | 213 ± 49 | - | - | - |
| 28 [a] | 31.4 | 356.24 | 207 ± 50 | - | - | - |
| 29 | 32.0 | 517.69 | 174 ± 79 | - | - | - |
| 30 | 25.0 | 656.40 | 136 ± 33 | 115 ± 11 | 0.393 | 1.19 |
| 31 | 24.2 | 530.75 | 117 ± 38 | - | - | - |
| 32 | 52.8 | 253.11 | 108 ± 83 | - | - | - |
| 33 | 31.4 | 988.64 | 98 ± 23 | - | - | - |
| 34 | 37.5 | 800.44 | 70 ± 27 | 61 ± 13 | 0.451 | 1.14 |
| 35 | 39.1 | 429.25 | 58 ± 10 | - | - | - |
| 36 | 16.0 | 245.23 | 53 ± 27 | - | - | - |
| 37 | 52.4 | 382.20 | 50 ± 10 | - | - | - |
| 38 | 20.4 | 842.28 | 47 ± 41 | 123 ± 56 | 0.367 | 0.38 |
| 39 | 32.1 | 633.74 | 33 ± 25 | - | - | - |
| 40 | 32.1 | 634.10 | 33 ± 4 | - | - | - |
| 41 | 26.3 | 961.47 | 26 ± 14 | - | - | - |
| 42 | 26.4 | 667.80 | 19 ± 9 | - | - | - |

[a] This peak overlapped with one of the adducts produced by reaction of oxidized arachidonic acid with ctDNA (data not shown); [b] This peak overlapped with one of the adducts produced by reaction of hydroxy radical with ctDNA (data not shown); [c] This peak overlapped with one of the adducts produced by reaction of oxidized linoleic acid with ctDNA (data not shown).